Mesoscale Simulation of Open Cellular Convection: Roles of Model Resolutions and Physics Parameterizations

Journal of Physics: Conference Series **2362** (2022) 012006 doi:10.1088/1742-6596/2362/1/012006

Mesoscale Simulation of Open Cellular Convection: Roles of Model Resolutions and Physics Parameterizations

Hai Bui[1], **Mostafa Bakhoday-Paskyabi**[1]

[1]Geophysical Institute, University of Bergen, Bergen, Norway

E-mail: hai.bui@uib.no

Abstract. The Open Cellular Convection (OCC) associated with cold air outbreaks is a common phenomenon over the North Sea where a large number of wind parks are presented. Thus, reliable numerical simulations of OCC events have great importance for offshore wind energy. We investigate the ability to simulate the OCC events using the Weather Research and Forecast (WRF) model with the ERA5 reanalysis data as initial and lateral boundary conditions and the OSITA data as the sea surface temperature. The domains were nested from 9 km as the outermost domain to 1 km as the innermost domain surrounding the Teesside wind farm located in the North Sea off the northeast coast of England. We simulated an OCC event in 2015 with three series of sensitivity numerical experiments of planetary boundary layer, microphysics, and radiation parameterizations. The model outputs were validated against the wind observation at the Teesside's meteorological mast. The results suggest that the planetary boundary layer schemes are the most sensitive during the events compared to other parameterization schemes. Futher more, a convective-resolved resolution is necessary for simulating the OCC variation properly. The paper also discuss the verification methods for such short time-scale events like the OCC.

1. Introduction

Open Cellular Convection (OCC) is a special type of mesoscale shallow convection that often occurs when a cold air mass moves over a warmer sea surface during a cold air outbreak event [1, 2]. The OCC-induced minutes-to-hours fluctuations in the wind speed in the boundary layer can greatly affect the operation of offshore wind farms [2, 3] and reliable numerical simulations of OCC events are needed. The challenge of the OCC simulation lies in its short spatial-temporal scale of the shallow convective systems, which have predictable timescales of only a few hours or less [4, 5]. In the perspective of mesoscale models, the sub-hour fluctuations are considered stochastic and the exact time and location of the convective cells are unpredictable. However, because the OCC is also associated with the large-scale environmental conditions, a mesoscale model is expected to be able to simulate the mean—or the deterministic aspect—and the statistics of stochastic aspects of the OCC. For this reason, we propose the separation of the deterministic and the stochastic signals for model validation.

The accuracy of mesoscale simulations depends on many factors such as the quality of the input data, model resolution, as well as the choice of physics parameterizations of, for example, the boundary layer, microphysics, etc. To the authors' knowledge, there exist no studies on

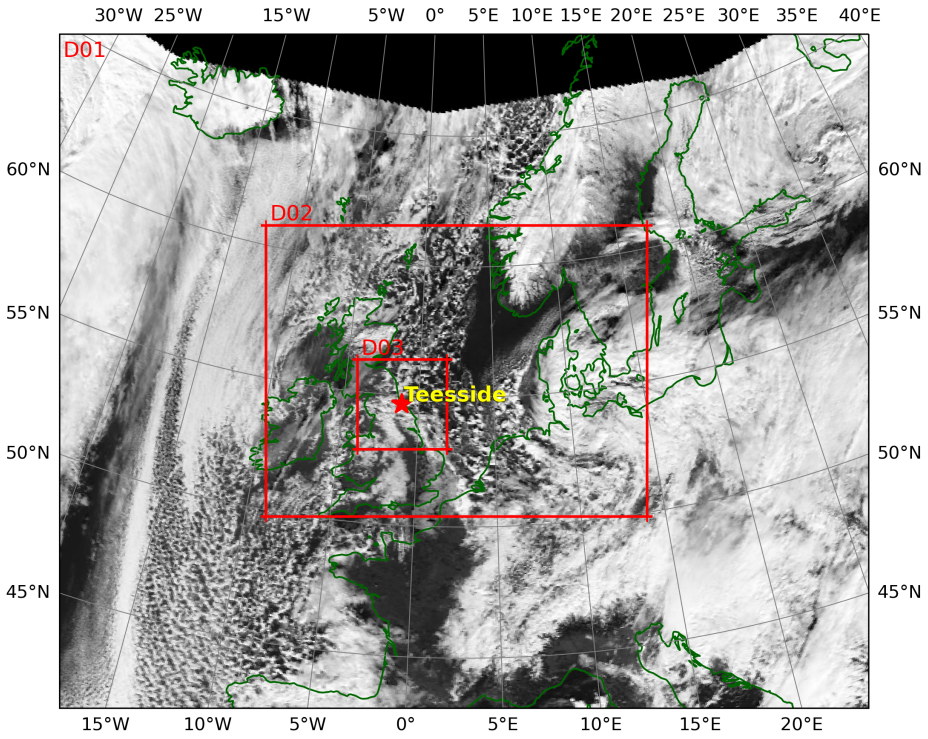

Figure 1. The WRF domains overlaid with the terra/MODIS satellite cloud image at 00Z, November 22, 2015, downloaded from https://wvs.earthdata.nasa.gov. The Teesside's meteorological mast is marked with the red star in the center of domain d03.

the physics parameterizations during the OCC events specifically. For the wind prediction in the boundary layer in general, several studies investigated the sensitivity of planetary boundary layer parameterizations on the wind speed [6, 7, 8, 9, 10, 11]. However, no agreement on the optimal schemes has been made.

In this study, we carried out a parameter sweep experiment of physics parameterization using the Weather Research and Forecast model (WRF) [12]. This paper investigates the sensitivity of the model resolution and physics options during an OCC event. Starting from a control experiment, we designed three series of experiments that modify the parameterizations of the planetary boundary layer, microphysics, and radiation (Section 2). We then validate the results against Teesside's meteorological mast data and derive the optimal configuration by combining the best option in each category (Section 3). The results emphasize the importance of the choice of physics parameterizations as well as model resolutions in the simulation of the OCC.

2. Model description and experiment design

2.1. Model description

We used the latest version of the Advanced Research WRF (ARW), version 4.3 with the main input data from the hourly ERA5 reanalysis [13] with the resolution of approximately 31 km. There nested domains (Fig. 1) are used: the first domain (d01) has the resolution of 9 km and covers a part of north-west Europe and a part of North Atlantic to downscale the large scale features from the reanalysis data; the second domain (d02) has a resolution of 3 km and covers the North Sea regions; and finally, the third domain (d03) centered around Teesside region with

Table 1. Experiment design. Option denoted by "-" means that it is the same as the control (ctrl) experiment.

Experiment	Boundary layer	Surface layer	Microphysics	Shortwave rad.	Longwave rad.
ctrl	MYNN2 [15]	MYNN	Thompson [16]	RRTMG [17]	RRTMG
bl01	YSU [18]	MM5 [19]	-	-	-
bl02	MYJ [20]	Eta [20]	-	-	-
bl04	QNSE [21]	QNSE	-	-	-
bl06	MYNN3 [22]	MYNN	-	-	-
bl07	ACM2 [23]	Pleim-Xiu[24]	-	-	-
bl08	BouLac [25]	MM5	-	-	-
bl09	UW [26]	Eta	-	-	-
bl10	TEMF [27]	TEMF	-	-	-
mp02	-	-	Lin [28]	-	-
mp04	-	-	WSM5 [29]	-	-
mp06	-	-	WSM6 [30]	-	-
mp07	-	-	Goddard [31]	-	-
mp10	-	-	Morrison [32]	-	-
mp13	-	-	SBU–YLin[33]	-	-
mp14	-	-	WDM5 [34]	-	-
mp16	-	-	WDM6 [34]	-	-
ra01	-	-	-	Dudhia [35]	RRTM [36]
ra02	-	-	-	Goddard [37]	RRTM
ra03	-	-	-	CAM [38]	CAM
ra04	-	-	-	New Goddard [39]	New Goddard

a resolution of 1 km and domain size of 384 km × 384 km. We use 60 stretched vertical levels with the highest resolution near the surface of about 10 m and 21 levels below the height of 500 m. Because of the importance of the Sea Surface Temperature (SST) and the land-sea distribution, we used the OSTIA SST reanalysis [14], which has a resolution of 0.054 degrees (or roughly 6 km), which is much higher than the ERA5's (31 km). The OSTIA SST is linearly interpolated from the daily frequency to an hourly basis to accommodate the ERA5.

The simulation is carried out for 2 days from 00Z November 21 to 00Z November 23, 2015. During the period, an OCC event occurred over the North Sea, and the convective cells were propagated through Teesside's meteorological mast. This OCC was triggered by the cold air outbreak that was associated with the cold air mass behind an extratropical cyclone, which was situated over North Germany at 00Z on November 22 (Fig. 1). We extract the simulations' output at the Teeside's mast location at every model time step, which are 30 seconds, 10 seconds, and 10/3 seconds for d01, d03, and d03 respectively.

2.2. Experiment design

There are several fundamental categories of physics parameterizations in the WRF: the Planetary Boundary Layer (PBL), the surface layer, the microphysics, the cumulus convection, the short wave radiation, and the longwave radiation (denoted by rad. in Table 1). Each category has a number of options for different parameterization schemes. The number of all combinations of different options is large and impractical for our study. However, some PBL and surface schemes, as well as short wave and long wave radiations, are designed to be used together. We

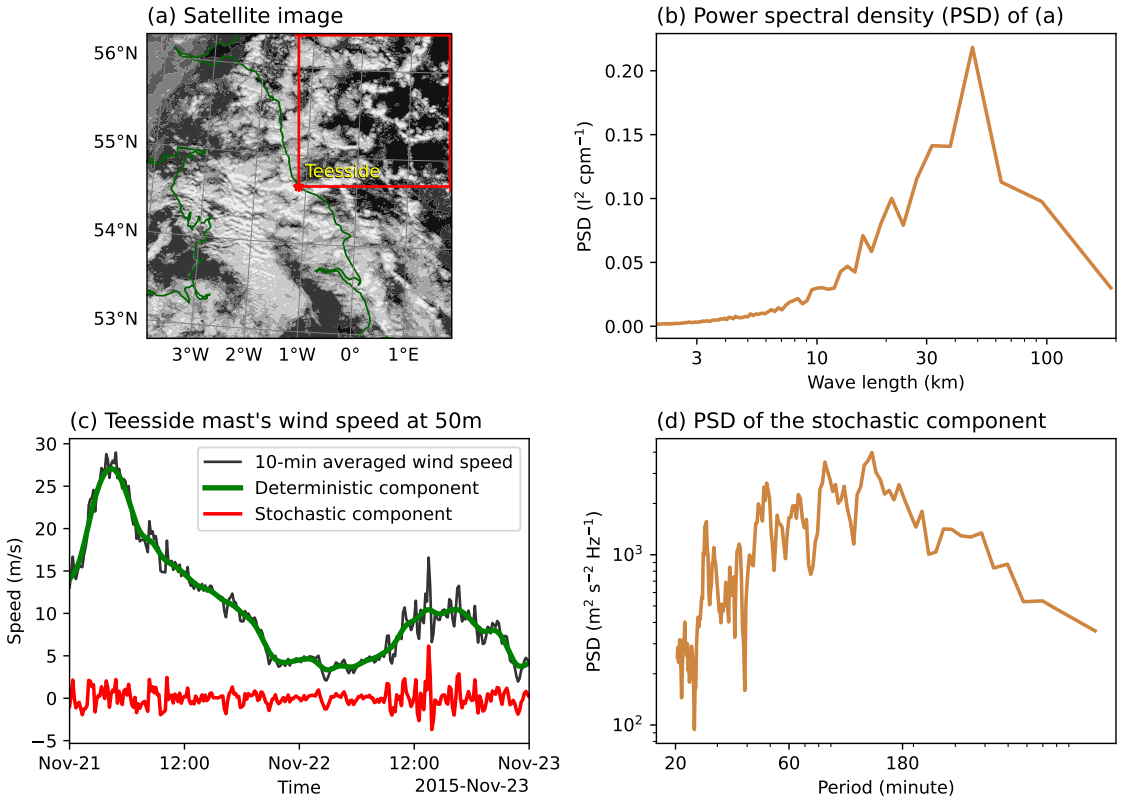

Figure 2. (a) Satellite image zoomed in to the d03 domain with the red box showing the region for the spectral analysis; (b) Averaged power spectral density (PSD) as a function of wave-number ($k = \sqrt{k_x^2 + k_y^2}$), here we convert the wave-number to wave-length ($\lambda = 2\pi/k$) for a more intuitive interpretation ; (c) 10-min average wind speed at 50 m of the Teesside's mast anemometer and the decomposition of the original signal into the deterministic and stochastic component; (d) PSD of the stochastic component in (c) as a function of fluctuation period.

can reduce the number of experiments by starting from a control (ctrl) one and varying the parameters in each parameterization category.

In this paper, the control experiment (Table 1) was obtained by using the WRF's built-in CONUS physics suite with the planetary boundary layer and surface layer schemes replaced by the MYNN schemes because of their popularity among wind energy applications [40, 41]. Starting from the control experiment, we arrived at 20 additional experiments in three categories (Table 1): eight experiments that vary the PBL - surface schemes, eight experiments that vary the microphysics schemes, and four experiments that vary the radiation schemes. We turned off the cumulus parameterization for the 3-km and 1-km domains because the convection is partly resolved at these resolutions. For the 9-km domain, the Tiedtke cumulus scheme [42] was used for all the experiments. For the land surface, we used the unified Noah land surface model [43]. We did not include the wind farm parameterization because it can only be used together with the MYNN planetary boundary layer schemes.

2.3. Validation method

Many previous studies [6, 7, 8, 10, 9, 11] for the wind simulation validate the simulated wind speed against the observations such as meteorological mast, lidar, etc. However, during OCC events, the stochastic nature of the minute to hour-scale fluctuations of the convective cell makes it impossible for the mesoscale model to predict the correct timing of those variations. Thus, we decomposed the time series of wind speed into deterministic and stochastic components. The deterministic component is calculated using the Locally Weighted Scatterplot Smoothing (LOWESS [44]) method with a bell-shaped weight function:

$$w^i = \exp\left[-\frac{(t^i - t)^2}{2/\tau^2}\right], \tag{1}$$

where t^i is the discrete time-step of the original signals and τ is the parameter that determines the smoothness of the curve, which takes the value of 30 minutes in this paper. The stochastic signal is then obtained by subtracting the deterministic signal from the original time series.

Figure 2c shows the 10-min averaged wind speed at the height of 50 m above the sea level from the cup anemometer at the Teesside's meteorological mast during the study period and the two decomposed components. The Power Spectral Density (PSD) of the fluctuations (Fig 2d) shows the peaks with the periods from 30–180 minutes (approximates 30, 50, 90, and 180 min). We applied the same procedure for the 10-min averaged wind speed extracted from the model output to validate against the observation. For the deterministic aspects, the Root Mean Square Error (RMSE) and correlation coefficient of the deterministic component were used to compare the output of the simulations with the observations. For the stochastic aspects, we compared the standard deviation of the stochastic component against the observation.

To characterize the horizontal scale of the OCC in the observation, we applied a 2-dimensional spectral analysis on the satellite cloud image at 00Z, November 22, 2015, in a squared box with a size of 190 km with the bottom left corner on the Teesside's mast (Fig. 2a). The box is chosen as a sub-region of the innermost domain so that the same procedure can also be applied to all simulations. Then the averaged PSD as a function of wavenumber ($k = \sqrt{k_x^2 + k_y^2}$) is calculated. For the observation, the horizontal scale of the OCC is about 50 km as indicated by the peak in the PSD in Fig. 2b.

3. Result

Figure 3 summarizes the main validation scores of our study. Regarding the role of the model resolution, we found that higher resolution does not lead to a better performance in terms of the deterministic aspects. It is interesting that for most of the cases, the in-between resolution, 3-km, performs the worst with the highest RMSE and lowest correlation coefficient. The 9-km resolution performs slightly better than the 1-km resolution. On the stochastic aspect, the standard deviation of the fluctuation is highly sensitive to the resolution with a higher value with higher resolution. The 9-km domain in all experiments roughly captures just about half of the observation's value, while most of the experiments can capture a realistic variation level at the 1-km resolution. To improve the simulation result, we first carry out a simple ensemble mean (named ens in Fig. 3). However, the result does not outperform other experiments in the deterministic sense, while the fluctuation of the OCC signal is heavily reduced (Fig. 3c).

Figure 3 also shows two experiments, com1 and com2 (Table 2), which are the combinations derived from choosing the options that perform well in each category. Experiment com1 is the combination of experiments bl08 (BouLac boundary layer), mp13 (SBU-YLIN microphysics), and ra01 (Dudhia and RRTM radiations), each performing the best in the deterministic aspect. However, bl08 and mp13 also have the lowest standard deviation of the fluctuation, which may result in an unrealistic variation of the wind speed during the OCC event. Thus, the com2

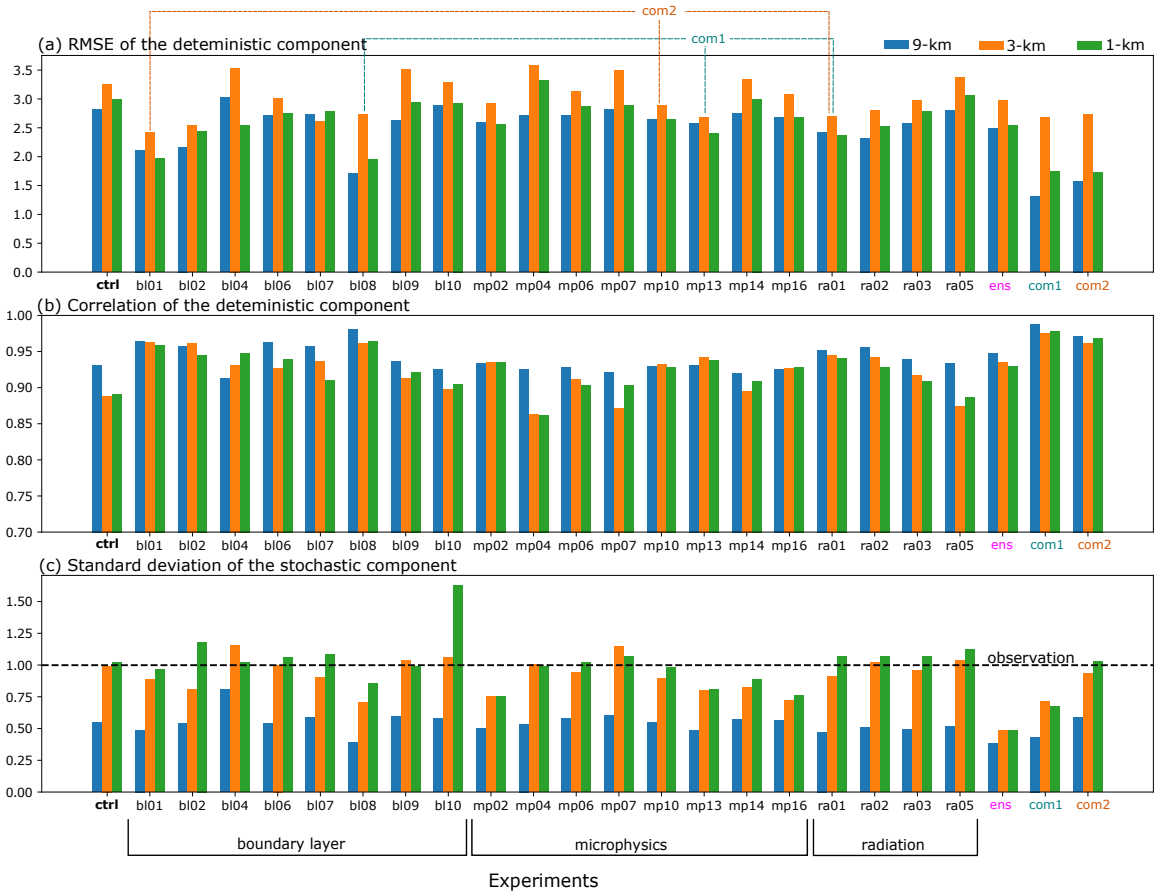

Figure 3. (a) Root mean square errors (RMSEs) and (b) correlation coefficients of the deterministic component of 10-m the height of 50 m compared against the Teesside's mast anemometer, (c) standard deviation of the stochastic component.

Table 2. Two derived combinations of physics configurations

Experiment	Boundary layer	Surface layer	Microphysics	Shortwave rad.	Longwave rad.
com1	BouLac	MM5	SBU–YLin	Dudhia	RRTM
com2	YSU	MM5	Morrison	Dudhia	RRTM

experiment is chosen from the experiments bl01 (YSU boundary layer) and mp10 (Morrison microphysics), which are the second-best in their category with a closer variation to the observation.

Experiment com1 performs better than all other experiments with the lowest RMSE and highest correlation at the 9-km and 1-km resolutions, which means the combination has an additive effect on the individual experiments. However, the fluctuation is also significantly reduced and is only slightly larger than the ensemble. On the other hand, com2 also performs well with a similar RMSE to com1 and a slightly lower correlation. However, the fluctuation

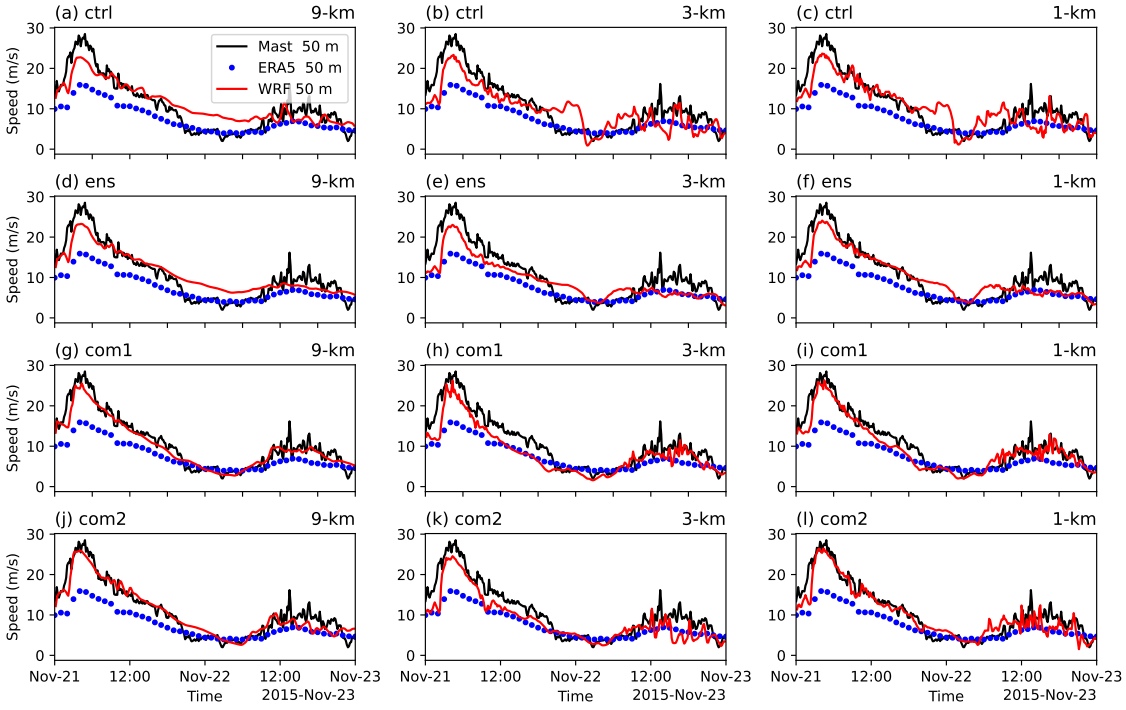

Figure 4. Time series of 10-min wind speed at 50 m above sea level from of the Teesside mast versus WRF simulations of experiments ctrl, ens, com1 and com2 at three resolutions. The hourly ERA5 data is also shown.

level of com2 is higher and is closer to the observation for the 1-km resolution.

Figure 4 shows the time series of 10-min averaged wind speed at the height of 50 m for experiments ctrl, ens, com1, and com2 and compared with the Teesside mast anemometer and the ERA5 reanalysis. All the simulations perform better than the forcing ERA5 data, which heavily underestimates the wind speed. Experiment ctrl underestimates the peak of the wind speed at the first 6 hours and overestimates the wind speed around 00Z on November 22 by about 5 m/s. Finer resolutions provide more realistic fluctuations, but the under/over-estimation persists. The ensemble mean, ens, does not improve the performance compared to the ctrl, and most of the fluctuation is removed for all resolutions.

Experiment com1, on one hand, gives the best result regarding deterministic component in all resolutions, especially 9-km. On the other hand, the short timescale fluctuation during the first day is heavily reduced, which explains the low standard deviation of the stochastic component in Fig. 3c. During the passage of the OCC on the second day, experiment com1 can capture some of the wind speed fluctuations for 3-km and 1-km resolutions, although the variation is still smaller than that of the observation.

Similar to com1, experiment com2 also performs similarly well despite different schemes of the boundary layer and microphysics parameterizations. Com2 performs better than com1 for the first day but slightly underestimates the wind speed for the last 6 hours of the period. The wind speed fluctuation level of com2 is closer to the observation than com1.

Figure 5 shows a snapshot of the vertical velocity at the Teesside turbines' hub height (80 m) for experiments ctrl, com1, and com2, and Figure 6a shows the characteristic length scale of the OCC by performing the spectral analysis on the vertical velocity. At 9-km resolution,

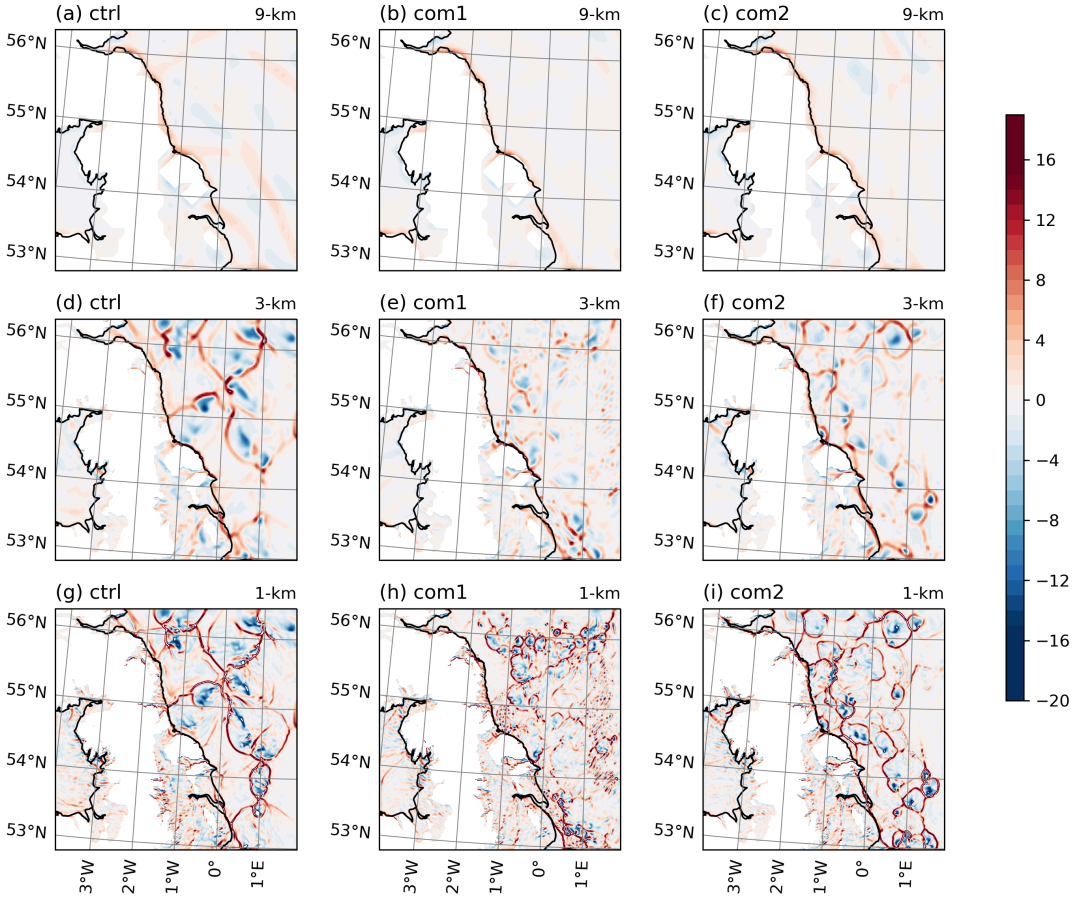

Figure 5. Snapshots at 12Z November 22, 2015 of vertical velocity at 80 m (Teesside turbine's hub height) in cm s^{-1} for experiments ctrl, com1, and com2. All plots are zoomed to the inner most domain (d03).

all experiments cannot resolve the OCC structure. At 3-km resolution and smaller, the OCC structure is revealed with upward motions at the edges and the downward motion in the center of the cells (Fig. 5d–i). The averaged power spectral density of the 80-m vertical velocity (Fig 6.a) shows that, for 3-km and 1-km resolutions, most of the experiments, except com1, have a realistic spatial scale ranging from 20 km to 70 km (compared to the 50-km scale of the observation in Fig. 2a). Experiment com1 has the smallest spatial scale, especially at 1-km resolution, where the spatial scale is less than one-fifth of the observation. The temporal power spectrum of wind speed (Fig 6.b) also shows higher resolution can capture fluctuation with higher frequencies. The peak periods of experiments ctrl and com2 range from two to three hours, similar to the observation (Fig. 2d). On the other hand, the peak period of experiment com1 is less than one hour.

4. Discussion and conclusion

This study investigated the ability of a mesoscale numerical model to simulate an OCC event that passed through Teesside's wind park in November 2015. We used the WRF model with three nested domains to downscale the ERA5 reanalysis to a 1-km resolution. Three series of parameter-sweep sensitivity experiments (Table 1) were tested to select optimal configurations

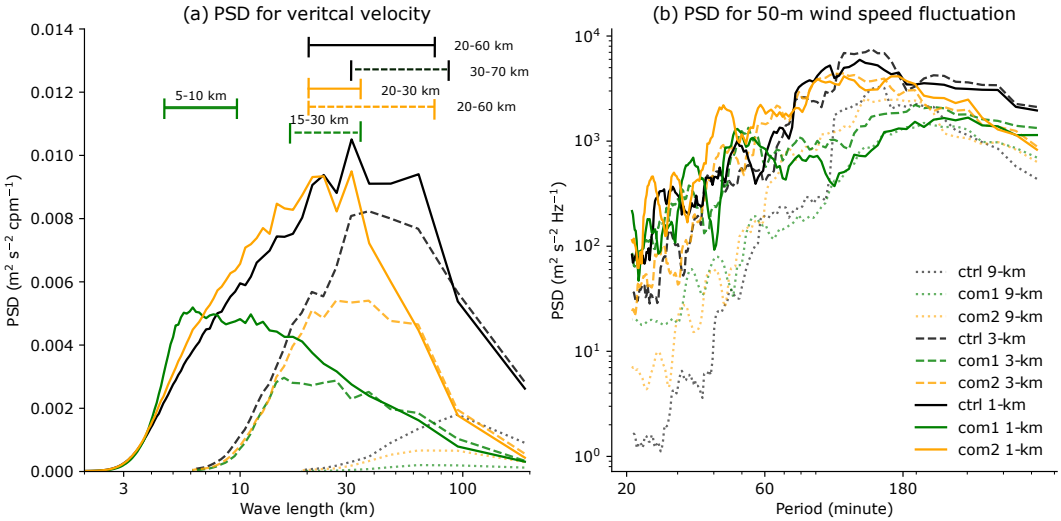

Figure 6. (a) Averaged power spectral density (PSD) of 80-m vertical velocity for experiments ctrl, com1, and com2; (b) PSD of 10-min wind speed fluctuations.

(Table 2) for the OCC event. To validate the model, we decomposed the time series into deterministic and stochastic components. The results show that model resolutions mainly affect the stochastic component rather than the deterministic component. Higher resolution results in higher wind speed fluctuation that is closer to the observation. The WRF model starts resolving the OCC structure from the resolution of 3 km and the spatial scale of the simulated OCC also strongly depends on the choices of the physics parameterization.

The MYNN schemes are popularly used in wind energy applications, partly because they can be used together with the wind farm parameterization [40, 41]. However, in this case study, both MYNN2 and MYNN3 did not perform well. We obtained two optimal configurations (Table 2) for the specific case. The first configuration performed the best in the deterministic aspect, however, the stochastic fluctuation is heavily damped. The second configuration performed well in the stochastic sense and is just slightly worse than the first configuration in the deterministic sense.

This study has an obvious caveat with only one case study, and the inaccuracy of the initial conditions and the observations are not taken into account. However, we demonstrated that an optimal configuration of physics parameterization can be obtained by first carrying out sensitivity studies of different parameterization categories. By combining the parameterization schemes from the well-performed experiments in each category, we obtained an optimal configuration that outperformed all individual experiments. To achieve a reliable general optimal configuration for OCC simulation, further studies are needed by using a larger number of cases, data assimilation, and additional sources of observation.

Acknowledgments

The work is a part of the HIghly advanced Probabilistic design and Enhanced Reliability methods for high-value, cost-efficient offshore WIND (HIPERWIND) project, which has received funding from the European Union's Horizon 2020 Research and Innovation Programme under Grant Agreement No. 101006689. The simulations were performed on resources provided by UNINETT Sigma2 - the National Infrastructure for High Performance Computing and Data Storage in Norway.

References

[1] Agee E M, Chen T and Dowell K 1973 *Bull. Am. Meteorol. Soc.* **54** 1004–1012
[2] Atkinson B and Wu Zhang J 1996 *Rev. Geophys.* **34** 403–431
[3] Göçmen T, Larsén X G and Imberger M 2020 *J. Phys. Conf. Ser.* **1618** 062014 ISSN 1742-6596
[4] Lorenz E N 1969 *Tellus* **21** 289–307
[5] Archer C, Simão H, Kempton W, Powell W B and Dvorak M 2017 *Renew. Energ.* **103** 346–360
[6] Draxl C, Hahmann A N, Peña A and Giebel G 2014 *Wind Energy* **17** 39–55
[7] Carvalho D, Rocha A, Gómez-Gesteira M and Santos C S 2014 *Appl. Energy* **135** 234–246
[8] Banks R F, Tiana-Alsina J, Baldasano J M, Rocadenbosch F, Papayannis A, Solomos S and Tzanis C G 2016 *Atmos. Res.* **176** 185–201
[9] Avolio E, Federico S, Miglietta M, Feudo T L, Calidonna C and Sempreviva A M 2017 *Atmos. Res.* **192** 58–71
[10] Gunwani P and Mohan M 2017 *Atmos. Res.* **194** 43–65
[11] De Lange A, Naidoo M, Garland R M and Dyson L L 2021 *Atmos. Res.* **247** 105214
[12] Skamarock W C, Klemp J B, Dudhia J, Gill D O, Liu Z, Berner J, Wang W, Powers J G, Duda M G, Barker D M *et al.* 2019 A description of the advanced research wrf model version 4 Tech. rep. National Center for Atmospheric Research: Boulder, CO, USA
[13] Hersbach H, Bell B, Berrisford P, Hirahara S, Horányi A, Muñoz-Sabater J, Nicolas J, Peubey C, Radu R, Schepers D *et al.* 2020 *Q. J. R. Meteorol. Soc.* **146** 1999–2049
[14] Stark J D, Donlon C J, Martin M J and McCulloch M E 2007 *Oceans 2007-europe* (IEEE) pp 1–4
[15] Nakanishi M and Niino H 2006 *Bound.-Layer Meteorol.* **119** 397–407
[16] Thompson G, Field P R, Rasmussen R M and Hall W D 2008 *Mon. Weather Rev.* **136** 5095–5115
[17] Iacono M J, Delamere J S, Mlawer E J, Shephard M W, Clough S A and Collins W D 2008 *J. Geophys. Res. Atmos.* **113**
[18] Hong S Y, Noh Y and Dudhia J 2006 *Mon. Weather Rev.* **134** 2318–2341
[19] Jiménez P A, Dudhia J, González-Rouco J F, Navarro J, Montávez J P and García-Bustamante E 2012 *Mon. Weather Rev.* **140** 898–918
[20] Janjić Z I 1994 *Mon. Weather Rev.* **122** 927–945
[21] Sukoriansky S, Galperin B and Perov V 2005 *Bound.-Layer Meteorol.* **117** 231–257
[22] Nakanishi M and Niino H 2009 *J. Meteorol. Soc. Jpn. Ser. II* **87** 895–912
[23] Pleim J E 2007 *J. Appl. Meteorol. Climatol.* **46** 1383–1395
[24] Pleim J E and Xiu A 1995 *J. Appl. Meteorol. Climatol.* 16–32
[25] Bougeault P and Lacarrere P 1989 *Mon. Weather Rev.* **117** 1872–1890
[26] Bretherton C S and Park S 2009 *J. Clim.* **22** 3422–3448
[27] Angevine W M, Jiang H and Mauritsen T 2010 *Mon. Weather Rev.* **138** 2895–2912
[28] Chen S H and Sun W Y 2002 *J. Meteorol. Soc. Jpn. Ser. II* **80** 99–118
[29] Hong S Y, Dudhia J and Chen S H 2004 *Mon. Weather Rev.* **132** 103–120
[30] Hong S Y and Lim J O J 2006 *Asia-Pac. J. Atmospheric Sci.* **42** 129–151
[31] Tao W K, Simpson J and McCumber M 1989 *Mon. Weather Rev.* **117** 231–235
[32] Morrison H, Thompson G and Tatarskii V 2009 *Mon. Weather Rev.* **137** 991–1007
[33] Lin Y and Colle B A 2011 *Mon. Weather Rev.* **139** 1013–1035
[34] Lim K S S and Hong S Y 2010 *Mon. Weather Rev.* **138** 1587–1612
[35] Dudhia J 1989 *J. Atmos. Sci.* **46** 3077–3107
[36] Mlawer E J, Taubman S J, Brown P D, Iacono M J and Clough S A 1997 *J. Geophys. Res. Atmos.* **102** 16663–16682
[37] Chou M D and Suarez M J 1994
[38] Collins W D, Rasch P J, Boville B A, Hack J J, McCaa J R, Williamson D L, Kiehl J T, Briegleb B, Bitz C, Lin S J *et al.* 2004 *NCAR Tech. Note NCAR/TN-464+ STR* **226** 1326–1334
[39] Suarez M J and Chou M d 1999 *NASA Tech. Memo. 104606* (Citeseer)
[40] Fitch A C, Olson J B, Lundquist J K, Dudhia J, Gupta A K, Michalakes J and Barstad I 2012 *Mon. Weather Rev.* **140** 3017–3038
[41] Giannakopoulou E M and Nhili R 2014 *Adv. Meteorol.* **2014**
[42] Zhang C, Wang Y and Hamilton K 2011 *Mon. Weather Rev.* **139** 3489–3513
[43] Mukul Tewari N, Tewari M, Chen F, Wang W, Dudhia J, LeMone M, Mitchell K, Ek M, Gayno G, Wegiel J *et al.* 2004 *Proceedings of the 20th Conference on Weather Analysis and Forecasting/16th Conference on Numerical Weather Prediction, Seattle, WA, USA* vol 14
[44] Cleveland W S and Devlin S J 1988 *J. Am. Stat. Assoc.* **83** 596–610